BNL-62016

JOURNAL OF GEOPHYSICAL RESEARCH, VOL. 101, NO. D22, PAGES 29,111–29,121, DECEMBER 20, 1996

Water-soluble fractions of aerosol and their relations to number size distributions based on aircraft measurements from the North Atlantic Regional Experiment

Shao-Meng Li, C. M. Banic, W. R. Leaitch, P. S. K. Liu, and G. A. Isaac
Atmospheric Environment Service, Downsview, Ontario, Canada

X.-L. Zhou and Y.-N. Lee
Brookhaven National Laboratory, Upton, New York

Abstract. Aerosol chemical and physical measurements were made at altitudes from 0.27 to 3 km near the coast of southern Nova Scotia, Canada, during the 1993 North Atlantic Regional Experiment. The volume distributions of aerosol with diameters between 0.005 and 3 μm were dominated by accumulation mode particles. The mass and volume ratios (R_m and R_v) of the sum of soluble organics (SumOrg) to non-sea-salt (nss) $SO_4^=$ were relatively invariant for estimated total particle mass (TPM) in excess of 13 μg m^{-3} (high TPM) but increased sharply with decreasing TPM below 13 μg m^{-3} (low TPM). Overall, the relationships between TPM and R_m and R_v were found to be $R_m = -(0.17 \pm 0.44) + (3.5 \pm 1.0)\mathrm{TPM}^{-(0.69\pm0.39)}$ and $R_v = -(0.35 \pm 0.70) + (5.7 \pm 1.7)\mathrm{TPM}^{-(0.68\pm0.39)}$. The high TPM aerosols originated in eastern North America and had average composition of 46% nss$SO_4^=$, 8% NH_4^+, and 8% SumOrg. In contrast, low TPM aerosols were found to be of background continental or marine tropospheric origins and had average composition of 23% nss$SO_4^=$, 9% NH_4^+, and 20% SumOrg. The aerosols in both TPM regimes were separated into two groups based on the mode of the volume distributions. The correlation between the mass of each species and the particle volume distribution was investigated for these groups.

1. Introduction

The role of aerosol particles in global climate change is being debated and quantified [*Charlson et al.*, 1992; *Schneider*, 1994; *Penner et al.*, 1994; *Barron*, 1995]. *Charlson et al.* [1991] demonstrated that the anthropogenic sulfate particles over eastern North America may have a direct radiative forcing of −(1–2) W/m^2 by scattering. The indirect radiative forcing of the sulfate particles by acting as cloud condensation nuclei (CCN) [*Charlson et al.*, 1992] is more difficult to quantify. Nevertheless, *Leaitch et al.* [1992] showed that there is a relationship between sulfate mass and cloud droplet number concentration and estimated that the indirect radiative forcing of sulfate particle over eastern North America is about −(2–3) W/m^2. However, a number of issues remain to be solved before the climate forcing by anthropogenic sulfate particles can be accurately assessed [*Penner et al.*, 1994], one of which is the role of organic matter in aerosol particles.

In general, sulfate accounts for only a fraction of the total aerosol particle mass, typically less than 50% even in polluted locations [*Heintzenberg*, 1989]. Organic matter can comprise an important and sometimes dominant fraction of aerosol mass, as shown, e.g., by *Novakov and Penner* [1993]. There is evidence that in remote atmosphere, part of the aerosol organic matter is in water-soluble organic species [*Andreae et al.*, 1988; *Talbot et al.*, 1990; *Li and Winchester*, 1993; *Kawamura and Usukura*, 1993; *Kawamura et al.*, 1995]. The water-soluble organic species may be good CCN, aid in the activation of insoluble particles, and contribute significantly to the total aerosol particle mass and volume. In addition, the chemical composition and physical characteristics of aerosol particles in the background troposphere and their climate forcing potential must be understood to serve as a reference point for assessing the contribution of anthropogenic aerosol to climate forcing.

The North Atlantic Regional Experiment (NARE) was carried out to investigate the transport of anthropogenic pollutants from eastern North America to the North Atlantic atmosphere [*Fehsenfeld et al.*, this issue]. This was an excellent opportunity to study anthropogenic aerosol particles downwind of major source areas in eastern North America and potentially to characterize the aerosol in the background continental and marine troposphere. Measurements of sulfate and organic species made in a wide range of conditions would yield a database suitable for assessing the relative importance of anthropogenic sulfate and the organic species.

In this paper, aerosol samples and particle size distributions taken at altitudes from 0.27 to 3 km are used to determine the relationship between aerosol particle physical and chemical properties. The mass of seven organic and six inorganic water-soluble species in the aerosol particles was quantified, and compared with the particle size distributions. The measurements may aid in determining the relative importance of these soluble species as CCN and in the scattering of radiation.

Copyright 1996 by the American Geophysical Union.

Paper number 96JD00345.
0148-0227/96/96JD-00345$09.00

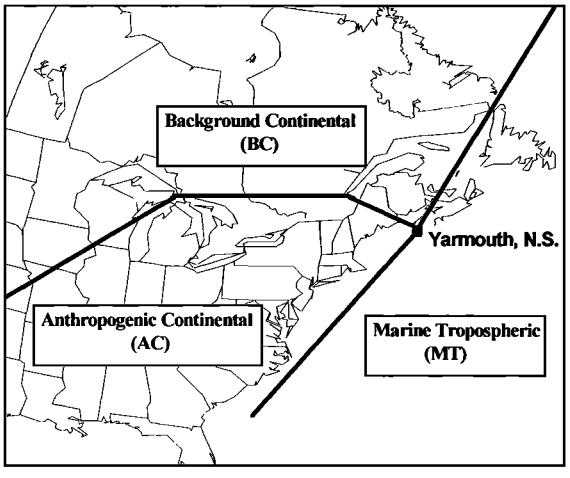

Figure 1. Location of the field experiment. Three air mass back trajectory categories are shown indicating air mass origins over background continental (BC) area, over marine troposphere (MT), and over anthropogenic continental (AC) pollution sources.

2. Method

2.1. Experiment

During the NARE intensive of August and September 1993 the National Research Council of Canada DHC-6 Twin Otter aircraft sampled aerosol particles at altitudes from 0.27 to 3 km within a 50-km radius of Yarmouth, Nova Scotia (Figure 1). Measurements characterizing the aerosol particles at the surface were made at Chebogue Point, 10 km south of Yarmouth, and the results are presented in a companion paper [*Liu et al.*, this issue].

Aerosol samples were collected using a filter pack through a forward facing, isokinetic stainless steel inlet, leading to a 5-cm internal diameter stainless sample line. The flow rates through the filters were set to match the flow through the inlet opening based on an airspeed of 60 m s^{-1}. During filter sampling the airspeed might have varied between 55 and 65 m s^{-1}. For reasonable variations in the velocity sampling ratio (i.e., inlet sampling velocity/aircraft velocity) during filter sampling, the analysis of *Radar and Marple* [1988] indicates that the impact of anisokinetic sampling on the particle concentration is <10% for submicron particles and <20% for the maximum particle size, 3 μm, measured with a particle measuring systems passive cavity aerosol spectrometer probe (PCASP-100X). The sampling of particles of larger size may be compromised by this approach; however, the measurements made with other electronic sampling probes indicate that the concentrations of these larger particles were not significant to the total aerosol volume.

Gelman Teflon filters, 47 mm in diameter, were used in the filter pack. Laboratory tests using a TSI CN counter downstream of the filter showed that these filters effectively trapped all particles >4 nm. In general, one or two samples were collected on most flights, each integrated over approximately 45 min at a single altitude between 0.27 and 3 km. The data set consists of 32 sampling periods characteristic of air masses without local impact. Approximately 1.5 m^3 of air were sampled for each filter. All concentrations are referred to 0°C and 1 atm.

Size distributions of dried aerosol particles (0.125–3 μm diameter) were determined in 15 size bins with the PCASP, which was calibrated before and after the experiment following a procedure as described by *Liu et al.* [this issue]. Tests have shown that when aerosol particles are sampled outside cloud, the particles are effectively dried due a low relative humidity of <10% in the probe [*Strapp et al.*, 1992]. Condensation nuclei (CN) concentrations (>0.005 μm) were measured with a TSI-3025 CN counter [*Kesten et al.*, 1991] sampling from a forward facing 0.8-cm ID stainless steel inlet line. The PCASP and CN data were recorded at 1 s resolution.

The filters were kept refrigerated at 4°C from the time of collection until extraction in 10-mL deionized water, followed by agitation in an ultrasonic bath for 1 hour. The extracts were then immediately analyzed for the organic anions formate (FOR), acetate (ACE), propionate (PRO), pyruvate (PYR), and methanesulfonate (MSA) using ion chromatography (IC) with a gradient method in which two-step concentrations in $Na_2B_4O_7$ eluent were used [*Li and Barrie*, 1993]. PYR was normally below the IC detection limit and hence not quantified. *Keene et al.* [1989] reported discrepancies in results on FOR and ACE in particles using several different procedures of storage and extraction, but the study was not conclusive with regard to what the causes of the discrepancies were. Our own experiences indicate that most of the degradation of the two carboxylic acids should occur in liquid phase, although filter storage and extraction procedure may play a role. It appears that our procedure is a variation of those used in the *Keene et al.* [1989] study. Hence the results on FOR and ACE obtained here may be subject to an unquantified level of uncertainties.

The same extracts were later analyzed with IC for oxalate ion (OXA) and the inorganic ions Cl^-, NO_3^-, and $SO_4^=$, using a carbonate/bicarbonate eluent, and Na^+, NH_4^+, K^+, Mg^{++} and Ca^{++} using a methanesulfonic acid eluent. Mg^{++} and Ca^{++} were identified in the sample extracts but were not different from their respective blank values. We expect the Cl^- results to be less reliable than the others because of the documented volatilization of HCl from sea-salt particles on filters by reacting with sulfuric acid particles while being sampled. The uncertainties in Cl^-, however, were not quantifiable using the filter pack sampling method.

Right after the extraction procedure, a small aliquot of each extract was transferred into a DNPH solution for analysis for carbonyl compounds using an HPLC method [*Lee and Zhou*, 1993]. Formaldehyde (HCHO), glyoxylic acid (GLYX), glycoaldehyde, and PYR were identified in the extracts, but only the first two were quantified. The IC and HPLC detection limits, in ppm of solution, are FOR, 0.008; ACE, 0.016; PRO, 0.011; OXA, 0.02; MSA, 0.012; HCHO, 0.005; GLYX, 0.015; Cl^-, 0.006; NO_3^-, 0.006; $SO_4^=$, 0.03; Na^+, 0.01; NH_4^+, 0.01; and K^+, 0.01. The air concentration detection limits depend on the air volume sampled and the filter blank level.

2.2. Data Processing

The 1 s PCASP and TSI data were averaged over the time periods of filter collection. The concentration of particles with diameter between 0.005 and 0.125 μm was calculated from the difference of the TSI and the total PCASP number concentrations. Total particle volume (TPV) for each filter sample was calculated by integrating the particle volume in each size range. The total particle mass (TPM) for each filter was calculated from the TPV and a composite density for each sample. This density was estimated as a weighted average of the densities of the measured chemical species as follows:

$$d = \sum m_k \Big/ \sum (m_k/d_k) \qquad (1)$$

where m_k is the measured mass of chemical species k and d_k is the corresponding density of this species. The ionic species were assumed to exist as salts and their densities d_k were found in the literature [*Lide*, 1992]. The value of d ranged from 1.31 to 1.79, decreasing as TPV decreased.

The underlying assumption is that d is not affected significantly by the presence of chemical species which are not quantified here. If species such as soot carbon [*Chylek et al.*, this issue], insoluble organic carbon, or crustal materials and other combustion products [*Li and Winchester*, 1990] were present, then the actual composite density for the aerosol particles would be different from that calculated. Nevertheless, this assumption is basically valid for two reasons: (1) most of the aerosol particle mass, as shown below, was measured; hence a small additional amount of unmeasured species will not lead to a significantly different composite density from that calculated using equation (1); and (2) we expect that some of the unmeasured species, such as soil particles and soot carbon with high density of approximately 2.0 g cm^{-3}, were balanced by insoluble organic species with lower densities. In fact, the relative contribution, as discussed below, of organic versus inorganic water-soluble species to total particle mass as derived using the composite density is quite insensitive to small amounts of additional mass with densities that can be reasonably assumed. The larger uncertainties in the calculation of TPM, we believe, came from the calibration of the PCASP: NaCl aerosols were used in the calibration but were only a small fraction of the observed aerosols. This will cause an uncertainty in the TPV because the refractive indices of the species in the aerosol particles may be different from that of NaCl. The largest uncertainties in the TPV are estimated to be about 20%.

3. Results

3.1. Air Concentrations of Water-Soluble Species

During NARE the Twin Otter sampled air masses with composition that ranged from near background to highly impacted by anthropogenic sources [*Banic et al.*, this issue; *Kleinman et al.*, this issue] and the data presented here for the aerosol samples reflect this difference in air masses. The air concentrations for the inorganic and organic species are shown as a function of altitude in Figure 2. The aerosol sampling frequently took place in pollutant plumes and the data in Figure 2 indicate the range of concentrations which were seen at the given altitudes. The data for PRO are not plotted since one third of the samples were below detection limit.

Non-sea-salt (nss) $SO_4^=$ was calculated using measured Na^+ as the tracer for sea salt and a mass ratio of $SO_4^=/Na^+ = 0.248$ based on the mean seawater composition [*Broecker and Peng*, 1982]. High $nssSO_4^=$ concentrations were seen at altitudes from

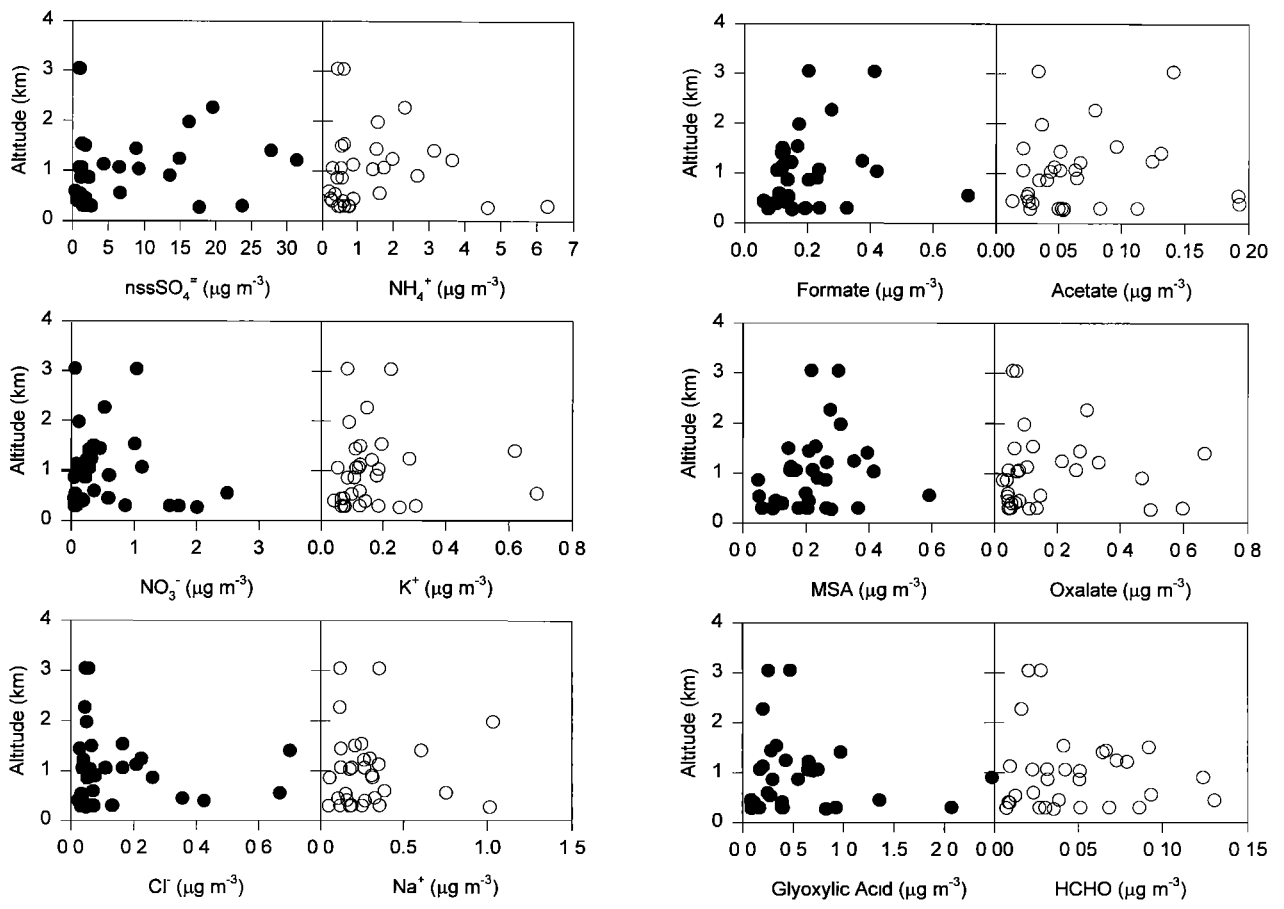

Figure 2. Vertical profiles of soluble species in aerosols during NARE: (left) inorganic species, (right) organic species.

Table 1. Summary Statistics of Air Concentrations (in $\mu g\ m^{-3}$) of Chemical Species, Sum of Inorganic Species, Sum of Organic Species, Total Particle Mass (TPM) (From PCASP Data), and Several Ratios Measured During NARE

	All Data		Low TPM (<13 $\mu g\ m^{-3}$)		High TPM (>13 $\mu g\ m^{-3}$)	
	Average	Median	Average	Median	Average	Median
Cl^-	0.14	0.065	0.13	0.073	0.15	0.06
NO_3^-	0.55	0.29	0.39	0.22	0.73	0.46
$ssSO_4^=$	0.075	0.063	0.057	0.063	0.094	0.067
$nssSO_4^=$	7.09	2.0	1.46	1.28	13.5	13.5
Na^+	0.29	0.25	0.23	0.25	0.37	0.26
NH_4^+	1.35	0.70	0.50	0.52	2.31	1.74
K^+	0.17	0.13	0.11	0.11	0.23	0.18
SumInorg	9.67	3.74	2.87	2.64	17.4	17.5
FOR	0.20	0.16	0.15	0.13	0.25	0.23
ACE	0.065	0.051	0.054	0.041	0.078	0.065
PRO	0.068	0.055	0.072	0.055	0.063	0.054
MSA	0.23	0.21	0.16	0.15	0.30	0.28
OXA	0.16	0.080	0.062	0.054	0.28	0.26
GLYX	0.58	0.39	0.41	0.36	0.78	0.65
HCHO	0.047	0.039	0.039	0.028	0.058	0.058
SumOrg	1.44	1.18	1.03	0.95	1.93	1.83
TPM (see text)	15.8	10.9	6.42	5.32	26.4	25.2
			Ratios SumOrg/nssSO$_4^=$			
Mass	0.62	0.48	0.91	0.85	0.29	0.20
Volume	0.94	0.65	1.42	1.33	0.38	0.27
			Mass Ratios to TPM			
SumOrg/TPM	0.14	0.12	0.20	0.15	0.08	0.06
$nssSO_4^=$/TPM	0.33	0.29	0.23	0.24	0.46	0.49
NH_4^+/TPM	0.084	0.071	0.085	0.067	0.083	0.080

0.27 to 2.2 km. Low $nssSO_4^=$ concentrations were also seen throughout the altitude range. The highest concentrations of NO_3^-, NH_4^+, Cl^-, Na^+, K^+, MSA, oxalate, glyoxylic acid, and HCHO were found below 1.5 km, with HCHO and glyoxylic acid near detection limit above 1.5 km, although the Cl^- data do not represent true sea-salt particle because of the expected reaction between sea salt and sulfuric acid particle which releases HCl. Again, both formate and acetate may be subject to uncertainties that are not quantified. But relatively speaking, they showed no obvious trend in concentration with altitude, but the maximum concentrations were within the marine boundary layer. For all inorganic and organic species the lowest concentrations were observed in the marine boundary layer, generally below 0.5 km. Even lower concentrations of the organics were seen at the surface [*Liu et al.*, this issue]. The general profiles indicate that transport both aloft and in the marine boundary layer was important for most of these organic species.

The mean and median of the concentrations for the inorganic species, and the seven organic species which were determined using the IC, are given in columns 1 and 2 of Table 1. FOR and ACE results apparently are with unknown levels of uncertainties due to storage and extraction procedures, and Cl^- should have a negative interference due to the sampling method as discussed earlier on. SumInorg and SumOrg refer to the sum of the inorganic and organic species given in the table. The dominant species is seen to be $nssSO_4^=$. The large difference between the mean and the median for $nssSO_4^=$ is due to high values which were seen on occasion (Figure 2). The second most abundant species was NH_4^+, followed by NO_3^-. The sea-salt species ($ssSO_4^=$, Na^+, K^+, Cl^-) were low overall. GLYX was the most abundant of the seven organic species, followed by MSA and FOR, but still much smaller in concentration than $nssSO_4^=$. Median and average concentrations of the organic species were similar to the inorganic sea-salt species and NO_3^-.

3.2. Mass and Volume Contribution of Water-Soluble Species

The scatterplot between $nssSO_4^=$ mass and TPM is shown in Figure 3 (left). For the low end of TPM the relationship is apparently different from that for the high end of TPM. The relationship was explored using an interactive linear regression analysis procedure as follows: for the low-end TPM data the data points were gradually included in the analysis with increasing TPM value, starting from the lowest TPM, to the interactive linear regression analysis until the percentage variance explained by the linear relationship (R^2) started to drop significantly, which occurred at TPM = 15 $\mu g\ m^{-3}$. This procedure yielded the relationship between $nssSO_4^=$ and TPM for the low TPM. For the high-end TPM values, a similar procedure was followed but starting from the highest TPM value, which yielded the relationship for the high TPM with the drop-off in R^2 at TPM = 9.8 $\mu g\ m^{-3}$. The crossover point of the two linear relationships, as shown in Figure 3 (left), occurred at TPM of approximately 13 $\mu g\ m^{-3}$. Hence two TPM regimes, TPM $< 13\ \mu g\ m^{-3}$ and TPM $> 13\ \mu g\ m^{-3}$, are referred to as low TPM and high TPM regimes, respectively, in the text below, although it is clear that the data points around this crossover point can be described equally well with either relationships. The two linear relationships have significantly different correlation coefficients and slopes for the two regimes: for the high TPM the regression yields a slope of 0.72 with intercept −5.4, suggesting that 72% of the increase in

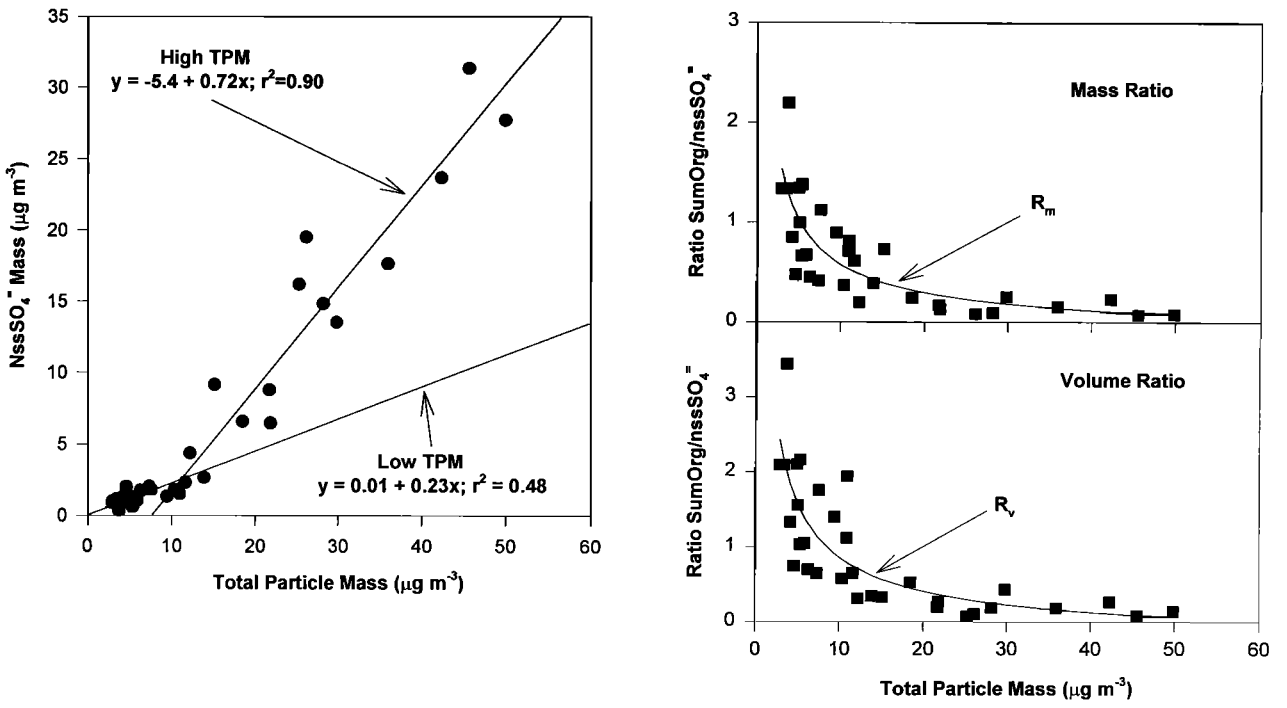

Figure 3. (Left) Relationship between $nssSO_4^=$ versus total particle mass. (Right) Relationship between mass and volume ratio of $SumOrg/nssSO_4^=$ versus total particle mass. The curves represent the best fit functions as follows: $R_m = -(0.17 \pm 0.44) + (3.5 \pm 1.0)TPM^{-(0.69 \pm 0.39)}$ and $R_v = -(0.35 \pm 0.70) + (5.7 \pm 1.7)TPM^{-(0.68 \pm 0.39)}$.

TPM above values seen in the low TPM regime are due to $nssSO_4^=$. For the low TPM the linear regression yields a slope of 0.23, with an intercept near zero, suggesting that approximately one quarter of the low TPM was accounted for by $nssSO_4^=$.

Table 1 also shows the average and median for the quantified species grouped by low or high TPM. With the exception of propionate, all species are seen at higher concentrations in the high TPM. This is especially true for $nssSO_4^=$ and to a lesser extent for NH_4^+, oxalate and NO_3^-. At high TPM the ratio $nssSO_4^=/TPM$ has an average of 0.46, indicating that about half the mass is accounted for by $nssSO_4^=$. For the low TPM regime, the contribution of $nssSO_4^=$ is about half of this, with the average ratio of $nssSO_4^=/TPM$ at 0.23. The NH_4^+ portion of TPM did not change from low to high TPM with the mass ratio NH_4^+/TPM near 0.08 in all aerosols. Hence $nssSO_4^=$ and NH_4^+ together accounted for 54% of the TPM in the high TPM regime and 32% of TPM in the low TPM regime, indicating that other compounds were relatively more important in the low TPM.

The ratio SumOrg/TPM averages 0.20 in the low TPM, similar to the $nssSO_4^=/TPM$ ratio, but only 0.08 in the high TPM. Hence, on average, SumOrg, $nssSO_4^=$, and NH_4^+ account for 62% of the high TPM and 52% of the low TPM. Here we define the total measured soluble mass (TMSM) as the sum of the mass of all chemical species which were measured. It includes all the individual species as listed in Table 1. The TMSM is 67% of the low TPM regime and 69% of the high TPM, based on the average of the TMSM/TPM ratio. The difference between the TPM and the TMSM can be due to other soluble species which were not quantified, such as other dicarboxylic acids [*Kawamura*, 1993; *Kawamura et al.*, 1995], insoluble species such as soot carbon [*Chylek et al.*, this issue], and soil dust. The difference can also be due to the uncertainty in the TPV (about 20%) and hence TPM caused by the uncertainties in the calibration of the PCASP.

The relative chemical composition of the aerosol particles as a function of TPM is demonstrated using the mass ratio $R_m = SumOrg/nssSO_4^=$. The average R_m was 0.91 for the low TPM and 0.29 for the high TPM (Table 1), and the relationship between R_m and TPM for individual samples, given in Figure 3 (right), illustrates a strong dependency of R_m on TPM. In the low TPM regime, R_m is variable but always greater than 0.3, with less variability and lower values seen for the high TPM. The best fit to the data in Figure 3 (right) gives

$$R_m = -(0.17 \pm 0.44) + (3.5 \pm 1.0)TPM^{-(0.69 \pm 0.39)},$$
$$R^2 = 0.67 \qquad (2)$$

On seven occasions, R_m exceeded 1, with a maximum of 2.3, indicating the importance of the soluble organics at low TPM.

The volume of the aerosol particles is important in determining the direct radiative properties. This is especially true for the volume partitioning in the submicron particle size range, where the Mie scattering is most effective. In the present study, no size distribution of the volumes of each individual species or a summation of the species can be determined, and hence the contributions of the individual species to the scattering are uncertain. However, the volume ratio of the organic species to $nssSO_4^=$, $R_v = SumOrg/nssSO_4^=$, has been determined and is shown as a function of TPM in Figure 3 (right). The volume of each organic species was determined from the measured mass and its density; the volume of $nssSO_4^=$ was calculated with a density of 1.8 g m^{-3}. The dependence of R_v on TPM is essentially the same as that for R_m, but the values

are about 60% higher. The best fit to the calculated R_v ratios in Figure 3 (right) is

$$R_v = -(0.35 \pm 0.70) + (5.7 \pm 1.7)\mathrm{TPM}^{-(0.68 \pm 0.39)},$$
$$R^2 = 0.67 \quad (3)$$

In the high TPM regime, R_v is below 0.5; in the low TPM regime it is well above 0.5 and approaches 3.5 at the lowest TPM. Thus the relative contribution of the soluble organics to the volume is greater than to the mass because of their low density.

3.3. Aerosol Size Distribution

The particle number concentrations for diameters between 0.005 and 3 μm were averaged over each filter collection period and the volume distributions $dV/d \log D$ were constructed for each sample. A principal component analysis (PCA) of the PCASP data [*Li et al.*, 1996] identified two major aerosol components for each of the low and high TPM regimes. The volume size distributions for the groups are shown in Figure 4. For both the low and the high TPM regimes the $dV/d \log D$ distributions of the first group (hereinafter aerosol 1) peaked at 0.21–0.26 μm, while for the second group (aerosol 2) the maximum shifted to 0.32–0.45 μm.

All four groups show a large contribution to the volume by accumulation mode aerosol at diameters between 0.15 and 0.5 μm. The high TPM aerosols have more volume in the accumulation mode sizes than the low TPM aerosols, with 20 μm^3 cm^{-3} the lower limit for the maximum $dV/d \log D$ in the high TPM and the upper limit for the maximum $dV/d \log D$ in the low TPM. The high TPM aerosols show a slight shift in the maximum $dV/d \log D$ toward larger particles than the low TPM aerosols. For example, high TPM aerosol 2 has a large fraction of volume in the 0.63- to 0.96-μm size range. Particles with sizes between 0.005 and 0.125 μm contribute negligible volume to the TPV and will not be included in the following analysis.

3.4. Correlations of Soluble Mass With Particle Size

Aerosol particles from all size classes were collected on a single filter, rather than fractionated by size. The relationship of the measured mass of a particular species to particle size can be investigated by looking for correlations between the mass and the volume in each size bin of the PCASP. The relationship for each chemical species with dV in each size bin of the PCASP was fit by linear regression, and the Pearson correlation coefficients R were determined. A significant coefficient of determination (R^2) indicates that a species covaried with dV in that particular size bin. The R^2 for the relationships for $nssSO_4^=$, NH_4^+, OXA, and GLYX, all significant at the 95% confidence level ($p < 0.05$), are shown in Figure 5. The R^2 for the other species were generally not significant at the 95% confidence level and are not shown. The mean $dV/d \log D$ distribution for each aerosol group is also shown.

The maximum correlations for $nssSO_4^=$ with dV are seen for the accumulation mode for the high TPM regime: for aerosol 1 the highest R^2 occur at 0.21–0.45 μm, while for aerosol 2, the R^2 are high over the wider range of 0.21–0.96 μm. Relatively high correlations for the low TPM regime occur for aerosol 2 at 0.21–0.45 μm (similar to high TPM aerosol 2 but at lower R^2 values), as well as for sizes <0.18 μm. The low TPM aerosol 1 has all R^2 below the $p < 0.05$ confidence level, but the tendency is similar to that of high TPM aerosol 1. The correlations indicate that much of the $nssSO_4^=$ mass is present in the accumulation mode. They also suggest that aerosols 1 and 2 may have undergone different atmospheric processes.

The correlations for NH_4^+ are remarkably similar to those of $nssSO_4^=$ in the high TPM and are generally similar in the low TPM. Two noticeable differences between NH_4^+ and $nssSO_4^=$ seen for the low TPM are (1) the R^2 are significant for low

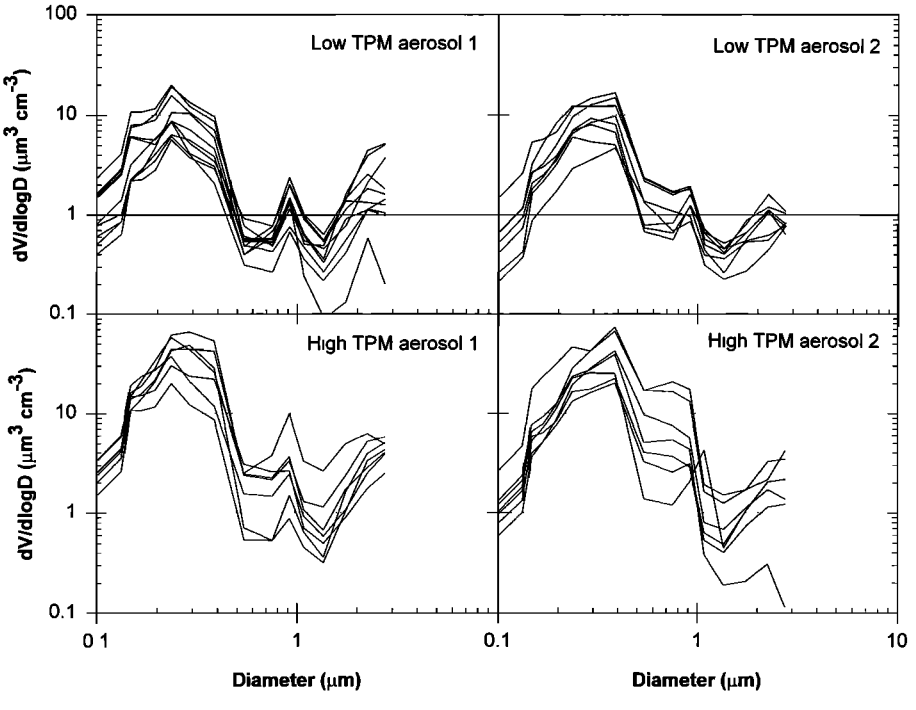

Figure 4. Volume size distributions for aerosols 1 and 2 of low total particle mass (TPM) regime (<13 μg m^{-3}) and high TPM regime (>13 μg m^{-3}).

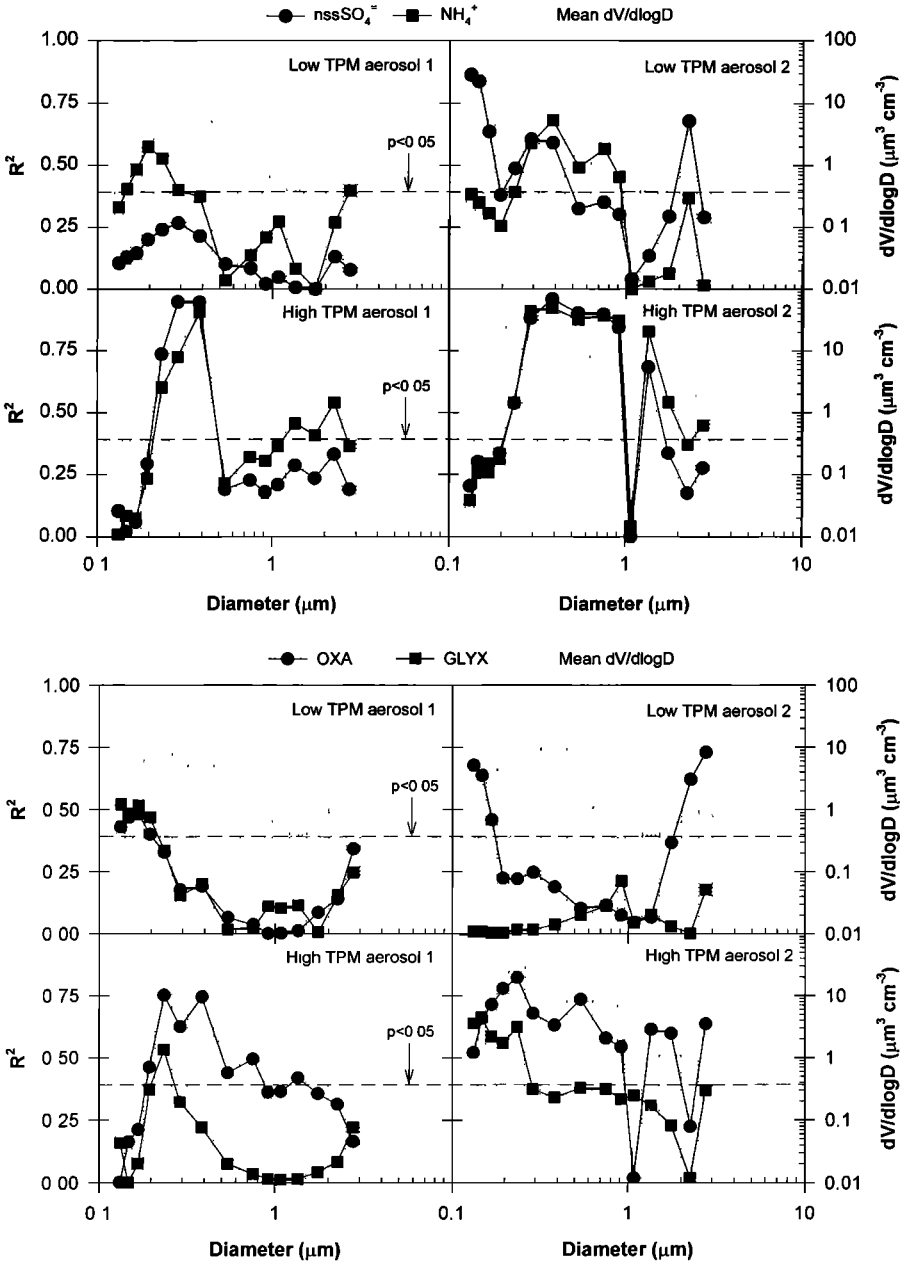

Figure 5. (Top) Coefficients of determination (R^2) of $nssSO_4^=$ and NH_4^+ with volume of particles in each size bin of the PCASP for low TPM aerosols 1 and 2 and high TPM aerosols 1 and 2, together with the mean volume size distributions for each aerosol. (Bottom) Similar to Figure 5 (top) but for OXA and GLYX.

TPM aerosol 1 at 0.14–0.32 μm for NH_4^+ but not for $nssSO_4^=$; and (2) the R^2 for NH_4^+ in the size range <0.18 μm for low TPM aerosol 2 are lower than for $nssSO_4^=$.

Significant correlations were found for OXA and GLYX in both TPM regimes (Figure 5 (bottom)), with OXA showing higher correlations than GLYX. For high TPM aerosol 1 the highest R^2 occur for OXA at 0.21–0.45 μm, the same size range as the most significant correlations were seen for $nssSO_4^=$. Significant correlations for OXA for high TPM aerosol 2 occur throughout the size range, with the maximum R^2 in smaller sizes than that for $nssSO_4^=$. The largest contrast between OXA and $nssSO_4^=$ occurs in the low TPM aerosols, where significant correlations for OXA are seen only for sizes <0.2 μm and at the largest sizes for aerosol 2. Significant correlations are seen for GLYX for high TPM aerosol 2 and low TPM aerosol 1 for particle sizes <0.2 μm and 0.21–0.26 μm for high TPM aerosol 1. Low TPM aerosol 2 do not correlate with GLYX. NH_4^+ was more highly correlated with volume at these sizes for low TPM aerosol 1 than was $nssSO_4^=$, indicating that NH_4^+ may be associated with the organic anions in these size ranges.

The R^2 given above provide an indication of the distribution of mass of the chemical species according to particle size. The results for OXA and GLYX suggest that these two species tend to present in smaller particles than $nssSO_4^=$. Similar results for OXA were reported for the ground level [*Liu et al.*, this issue].

3.5. Air Mass Back Trajectories

The three-dimensional 5-day back trajectories, calculated according to the method of *Olson et al.* [1978], have been categorized by *Banic et al.* [this issue] as having originated in one of three sectors shown in Figure 1: background continental (BC), anthropogenic continental (AC), and marine troposphere (MT). Inspection of the back trajectories for the times and altitudes of filter sampling shows that the aerosol were collected in air masses of different origins. It is possible that the differences seen in the chemistry of low and high TPM aerosol may be understood in terms of these air mass origins.

The air mass origin, altitude of collection, and TPM are given in Table 2 for each filter sample. The back trajectories for the high TPM aerosol show strong potential for recent influence of the anthropogenic pollution sources in eastern North America, whereas for the low TPM aerosol the air has traversed the marine troposphere or the clean continental region. Typical trajectories for the AC, BC, and MT categories are shown in Figure 6 for three examples: (1) The high TPM regime, sample TO46, was collected at 1246 m on September 7 at 1900 GMT, with the most applicable trajectories at 925 and 850 mbar. This shows the air mass traversed much of the pollution sources in the industrialized regions in eastern North America. (2) For the low TPM sample TO15-2, collected at 3048 m on August 17, at 1700 GMT, the air mass back trajectories starting at 700 mbar are applicable, for which little impact from pollution is expected. (3) For the low TPM sample TO18, collected at 447 m on August 19 at 1700 GMT, the 1000- and 925-mbar trajectories are applicable, which had primarily marine tropospheric influences.

Table 2. Summary of Categorization of the Filter Samples

Sample	Altitude	TPM	Category	TPM Regime and Aerosol
TO15-2	3048	2.9	BC	low, aerosol 1
TO27-2	3043	3.43	BC	low, aerosol 2
TO31-1	593	3.67	BC	low, aerosol 2
TO19	867	4.17	MT	low, aerosol 1
TO18	447	5.31	MT	low, aerosol 2
TO40	293	4.59	MT/AC	low, aerosol 2
TO5-1	1061	4.93	MT	low, aerosol 2
TO17	1061	5.05	MT	low, aerosol 1
TO14	393	6.3	BC/MT	low, aerosol 1
TO31-2	405	5.32	MT	low, aerosol 2
TO16	534	5.84	MT	low, aerosol 1
TO36	296	7.33	BC	low, aerosol 2
TO15-1	443	7.56	MT/BC	low, aerosol 1
TO28-2	1539	9.41	BC/AC	low, aerosol 2
TO13	1503	10.36	BC	low, aerosol 1
TO11	1129	12.19	AC/MT	low, aerosol 1
TO27-1	300	10.9	AC	high, aerosol 1
TO44	863	11.62	AC	high, aerosol 1
TO28-1	299	10.94	AC	high, aerosol 2
TO12	289	13.86	BC	high, aerosol 1
TO34	1036	15.12	AC	high, aerosol 1
TO26	553	18.48	AC	high, aerosol 1
TO32-2	1443	21.69	AC	high, aerosol 2
TO24	1068	21.84	AC	high, aerosol 2
TO48	1978	25.25	AC	high, aerosol 1
TO35	2271	26.08	AC	high, aerosol 1
TO46	1246	28.15	AC	high, aerosol 2
TO25	906	29.79	AC	high, aerosol 2
TO30	270	35.93	AC	high, aerosol 2
TO29	299	42.29	AC	high, aerosol 2
TO37	1220	45.56	AC	high, aerosol 1
TO33-1	1409	49.87	AC	high, aerosol 1

BC, background continental; MT, marine troposphere; AC, anthropogenic continental. Category summarized as in the work of *Banic et al.* [this issue].

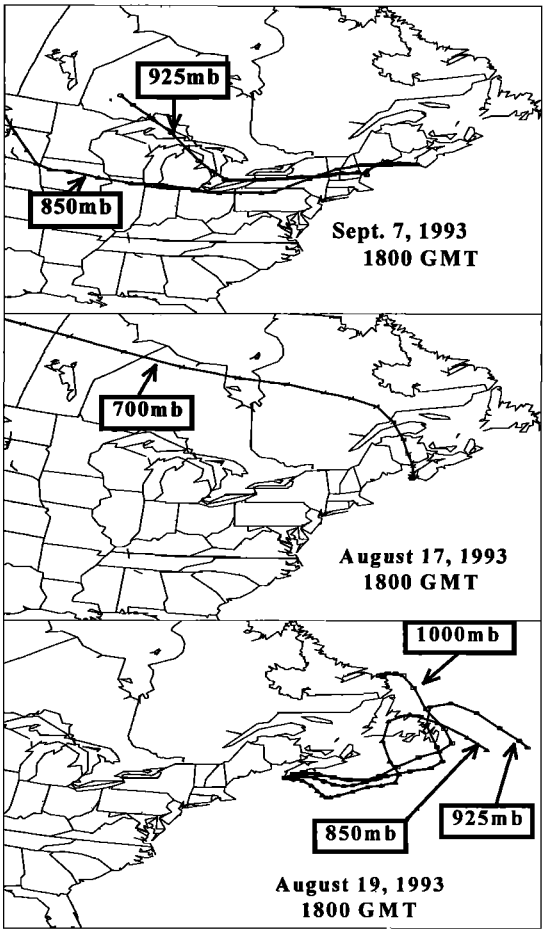

Figure 6. Typical cases for air mass back trajectories from (top) AC sector, (middle) BC sector, and (bottom) MT sector.

Basically, the air mass back trajectories for each filter sample were categorized similarly as one of the three examples. The three distinctively different origins had strong impact on the aerosol masses and their chemical compositions. For the high TPM aerosols the trajectories were mostly impacted by anthropogenic pollution. This anthropogenic impact is also reflected in the aerosol composition with an $nssSO_4^=$ content of 46% of TPM on average. In contrast, the low TPM aerosols were mostly originated over northern continental regions of Canada or over the marine troposphere. The lower $nssSO_4^=$ content in the low TPM aerosols (23% of TPM) is a reflection of the less influence from anthropogenic sources in these regions and may hence be regarded as more representative of the background aerosols.

4. Discussion

The above analyses yield several important results. First, for background continental or marine tropospheric air masses with little or no anthropogenic input the TPM was low, with $nssSO_4^=$ and the water-soluble organic species accounting for, on average, 23 and 20% of the TPM, respectively. The contribution from the sum of the water-soluble organics GLYX, OXA,

HCHO, PRO, ACE, FOR, and MSA to aerosol particle mass and volume was comparable to and often exceeded that from $nssSO_4^=$. However, it is not clear from the present analysis what the size distribution of this organic mass and volume is.

Second, high TPM aerosols were seen in air masses with potentially strong anthropogenic input from source regions in eastern North America, with $nssSO_4^=$ the dominant contributor to the mass. MSA is also higher in these high TPM aerosols than in low TPM aerosols, suggesting that biogenic $nssSO_4^=$ should be higher in these aerosols as well. However, compared to anthropogenic $nssSO_4^=$, biogenic $nssSO_4^=$ is negligible for this region [*Li et al.*, 1996]. The regression shown in Figure 3 for the relationship between $nssSO_4^=$ and TPM indicates that 72% of the particle mass of anthropogenic origin added to a background aerosol, defined as TPM $< 13\ \mu g\ m^{-3}$, consists of $nssSO_4^=$. A similar regression analysis for NH_4^+ shows that this species accounts for 10% of the added mass. In the high TPM aerosols, consisting of the background component and the anthropogenic addition, the $nssSO_4^=$ together with NH_4^+ contribute 54% of the mass. The mean mass and volume ratios of SumOrg/$nssSO_4^=$ for the high TPM aerosols were seen to be 0.29 and 0.38, respectively, and so the organic species are still important.

Third, the mass and volume ratios of SumOrg/$nssSO_4^=$ appear to be functions of TPM which can be reasonably summarized with equations (2) and (3). If these relationships are verified in other geographical locations and other seasons, then they provide a convenient parameterization relating the burden of organics to that of sulfate, which can be used in climate models.

Fourth, both high and low TPM regimes show significant correlations of particle volumes in some size ranges with $nssSO_4^=$. For the high TPM the correlations are highly significant especially in the accumulation mode, consistent with its dominant contribution to this aerosol. This is true also for the low TPM aerosol, although the statistics are not so convincing, consistent with the lower $nssSO_4^=$ mass fraction for these aerosols. The low and high TPM aerosols could be divided into two populations with different particle volume distributions. The high TPM aerosol 1 mass peaked at 0.21–0.26 μm, and its correlation with $nssSO_4^=$, indicates nucleation and accumulation mode $nssSO_4^=$. In comparison, aerosol 2 mass peaked at 0.32–0.45 μm, with a significant fraction of mass at 0.45–0.96 μm (Figure 4). At the same time, the correlation of aerosol 2 with $nssSO_4^=$ mass was strong for these size ranges (Figure 5 (top)), strongly suggesting that at least part of the mass at 0.45–0.96 μm in aerosol 2 was due to $nssSO_4^=$. One of the atmospheric processes for $nssSO_4^=$ to be present in this size range is the processing through stratus clouds [*Hoppel et al.*, 1986] and may have been responsible for the mass at 0.45–0.96 μm of aerosol 2. Although no other aircraft data exist to suggest that aerosol 2 had undergone stratus cloud processing, observations made at the Chebogue Point site indicated that in many cases the ground level aerosol had indeed been processed by marine stratus [*Liu et al.*, this issue], resulting in size distribution that is similar to those as seen in aerosol 2. For low TPM aerosols, only accumulation mode $nssSO_4^=$ was indicated from the correlations with the aerosols in each PCASP size bin.

It is not clear from the statistical analysis where the organic species are distributed in the size spectrum and whether they exist in external mixture with $nssSO_4^=$. Some of the organic species, notably OXA and GLYX, were most strongly associated with the smaller accumulation-mode particles (i.e., <0.3 μm) than was $nssSO_4^=$. Our newest airborne study in the same region in summer 1995, using a size-segregated aerosol sampler, confirmed such a size distribution. The correlations of the organic species with particle size for low TPM aerosols do not indicate a strong association with the main volume of the accumulation mode, inconsistent with the increasing importance of the organic species at low TPM. This may be due to the high variability in SumOrg/$nssSO_4^=$ and SumOrg/TPM at low TPM, and underscores the difficulty in using this type of analysis to represent the actual size distribution of chemical species.

The fact that organic species were relatively abundant in aerosol particles transported from areas of low anthropogenic impact suggests that aerosol particle radiative properties cannot be realistically modeled on a global basis by considering sulfate alone. In particular, the impact of these organic species on the particle volume is much higher than $nssSO_4^=$ for the same mass due to their lower densities. Equations (2) and (3) indicate that as the atmospheric particle loading decreases to background levels, the importance of organic species relative to sulfate increases drastically. The additional volume due to these water-soluble organic species can increase the total number of aerosol particles and/or increase the volume of particles containing sulfate and thus affect the direct radiative properties of the aerosol.

The indirect radiative forcing of aerosols may be enhanced if the CCN are increased by the presence of these water-soluble organic species. In general, because the organic anions in aerosol particles are hygroscopic, they can be effective CCN. The light-weight aldehydes are also highly soluble in water, and their presence in aerosol particles will facilitate the activation of the particles in cloud, especially if they are present on the surface of particles composed of insoluble organic compounds and elemental carbon, much like the activation of such particles due to coating of sulfuric acid [*Wyslouzil et al.*, 1994]. There is evidence that organic carbon aerosol particles may be more effective CCN than $nssSO_4^=$ [*Novakov and Penner*, 1993], possibly because of the presence of water-soluble organic species such as quantified here. In support of this result, *Liu et al.* [this issue] observed a highly significant correlation between particulate OXA and CCN activated at 0.4% supersaturation during NARE.

One possible reason for the importance of the organic species in the background aerosol is that they result from anthropogenic aerosols evolved through preferential removal of sulfate. This could occur if sulfate was initially associated with larger particles than the organic species, as indicated above. Such an association enhances the potential for activation of sulfate in cloud and its removal by precipitation as well as by dry deposition. A second possibility is that natural sources of these organic species over the continents and ocean are more prevalent than natural sources of sulfate. Sources of these species are the oxidation in the atmosphere of natural biogenic hydrocarbon emissions and natural biomass burning. For our understanding of the impact of the aerosols on climate it is critical to understand the sources, behavior, and sinks for these and other organic species in aerosol particles.

5. Summary

Aircraft measurements made during August and September 1993 as part of NARE indicated that the concentration of water-soluble organic and inorganic species in aerosol particles

sampled at 0.27 to 3 km were on average much higher than at ground level. Back trajectory analysis indicated transport to these altitudes from anthropogenic source regions, as well as areas which could give rise to continental and marine background aerosol. The organic species formate, acetate, propionate, methanesulfonate, glyoxylic acid, and formaldehyde accounted for a significant portion of the total particle mass (TPM).

Two regimes in TPM were identified, low TPM (<13 μg m^{-3}) and high TPM (>13 μg m^{-3}). $NssSO_4^=$ accounted for 46% of the TPM on average in the high TPM regime but only 23% of the TPM in the low TPM regime. SumOrg was 20% of low TPM on average and 8% of high TPM. NH_4^+ was 8% of the TPM in both regimes. The mass ratio SumOrg/$nssSO_4^=$ (R_m) was a function of TPM, with high values approaching 2 at the lowest TPM, dropping to about 0.15 for the high TPM. The best fit function is

$$R_m = -(0.17 \pm 0.44) + (3.5 \pm 1.0)\mathrm{TPM}^{-(0.69\pm0.39)}$$

Similarly, the volume ratio of SumOrg/$nssSO_4^=$ (R_v) was dependent on TPM, with high values near 3 at the lowest TPM, decreasing to approximately 0.3 for high TPM. The best fit function is

$$R_v = -(0.35 \pm 0.70) + (5.7 \pm 1.7)\mathrm{TPM}^{-(0.68\pm0.39)}$$

The increase in particle mass and volume due to the presence of these soluble organic species should increase the direct and indirect radiative cooling effect of aerosols from that due to sulfate alone. It is clear from the volume ratios that the total of the organics measured in this study can have a higher impact than $nssSO_4^=$ in background aerosol.

Two aerosol populations were found in each of the two TPM regimes, suggesting that some of the aerosol sampled may have been processed through clouds, such that $nssSO_4^=$ and oxalate mass was added to accumulation mode particles greater than 0.2 μm in size.

The regressions of the organic species with volume in each size bin of the PCASP show that oxalate and $nssSO_4^=$ were significantly correlated with the accumulation mode aerosol but oxalate with smaller sizes than $nssSO_4^=$, indicating that the two species were in external mixture. The correlations also indicate that glyoxylic acid was also present in particles of <0.26 μm.

Air mass back trajectories show that almost all low TPM aerosol were from either background continental or marine tropospheric regions, indicating general background aerosol particles, while all high TPM aerosols originated over anthropogenic pollution sources in eastern North America. Anthropogenic pollution-derived $nssSO_4^=$ particles have a dominant effect on aerosol mass in regions of significant anthropogenic impact. However, in the low TPM background aerosol the soluble organic species contribute comparable mass and volume to $nssSO_4^=$. Global modeling of the radiative role of aerosol in remote areas should consider the chemical composition of the aerosol, including both $SO_4^=$ and the organics.

Acknowledgments. The authors wish to thank the following: Helena Dryfhout for assistance in the chemical analyses; the staff of the IAR of the National Research Council of Canada for the operation of the Twin Otter research aircraft; Steve Bacic for assistance in the field and Mark Couture for assistance in data processing; and the anonymous reviewers for useful suggestions.

References

Andreae, M. O., R. W. Talbot, T. W. Andreae, and R. C. Harriss, Formic and acetic acid over the central Amazon region, Brazil, 1, Dry season, *J. Geophys. Res.*, *93*, 1616–1624, 1988.

Banic, C. M., W. R. Leaitch, G. A. Isaac, M. D. Couture, L. I. Kleinman, S. R. Springston, and J. I. MacPherson, Transport of ozone and sulfur to the North Atlantic atmosphere during NARE, *J. Geophys. Res.*, this issue.

Barron, E. J., Global change researchers assess projections of climate change, *Eos Trans. AGU*, *76*(18), 185–190, 1995.

Broecker, W. S., and T.-H. Peng, *Tracers in The Sea*, pp. 26–27, Lamont-Doherty Geol. Obs., Columbia Univ., New York, 1982.

Charlson, R. J., J. Langner, H. Rodhe, C. B. Leovy, and S. G. Warren, Perturbation of the northern hemisphere radiative balance by backscattering from anthropogenic sulfate aerosols, *Tellus*, *43AB*, 152–163, 1991.

Charlson, R. J., S. E. Schwartz, J. M. Hales, R. D. Cess, J. A. Coakley Jr., J. E. Hansen, and D. J. Hofmann, Climate forcing by anthropogenic aerosols, *Science*, *255*, 423–430, 1992.

Chylek, P., C. M. Banic, P. A. Damiano, G. A. Isaac, B. Johnson, W. R. Leaitch, P. S. K. Liu, D. Ngo, F. Said, S. R. Springston, and B. Winter, Black carbon: Atmospheric concentrations and cloud water content measurements over southern Nova Scotia, *J. Geophys. Res.*, this issue.

Fehsenfeld, F. C., M. Trainer, and D. D. Parrish, Transport of O_3 and O_3-precursors from anthropogenic sources to the North Atlantic, *J. Geophys. Res.*, this issue.

Heintzenberg, J., Fine particles in the global atmosphere: A review, *Tellus*, *41B*, 149–160, 1989.

Hoppel, W. A., G. M. Frick, and R. E. Larson, Effect of nonprecipitating clouds on the aerosol size distribution, *Geophys. Res. Lett.*, *13*, 125–128, 1986.

Kawamura, K., Identification of C_2-C_{10} ω-oxocarboxylic acids, pyruvic acid, and C_2-C_3 α-dicarbonyls in wet precipitation and aerosol samples by capillary GC and GC/MS, *Anal. Chem.*, *65*, 3505–3511, 1993.

Kawamura, K., and K. Usukara, Distributions of low molecular weight dicarboxylic acids in the North Pacific aerosol samples, *J. Oceanogr.*, *49*, 271–283, 1993.

Kawamura, K., H. Kasukabe, O. Yasui, and L. A. Barrie, Production of dicarboxylic acids in the arctic atmosphere at polar sunrise, *Geophys. Res. Lett.*, *22*, 1253–1256, 1995.

Keene, W. C., et al., An intercomparison of measurement systems for vapor and particulate phase concentrations of formic and acetic acids, *J. Geophys. Res.*, *94*, 6457–6471, 1989.

Kesten, J., A. Reineking, and J. Porstendorfer, Calibration of a TSI model 3025 ultrafine condensation particle counter, *Aerosol Sci. Technol.*, *15*, 107–111, 1991.

Kleinman, L. I., P. H. Daum, Y.-N. Lee, S. R. Springston, L. Newman, W. R. Leaitch, C. M. Banic, G. A. Isaac, and J. I. MacPherson, Measurement of O_3 and related compounds over southern Nova Scotia, I, Vertical distributions, *J. Geophys. Res.*, this issue.

Leaitch, W. R., G. A. Isaac, J. W. Strapp, C. M. Banic, and H. A. Wiebe, The relationship between cloud droplet number concentrations and anthropogenic pollution: Observations and climatic implications, *J. Geophys. Res.*, *97*, 2463–2474, 1992.

Leaitch, W. R., C. M. Banic, G. A. Isaac, M. D. Couture, P. S. K. Liu, S.-M. Li, L. I. Kleinman, P. H. Daum, and J. I. MacPherson, Chemical and physical observations in marine stratus during the 1993 NARE: Factors controlling cloud droplet number concentrations, *J. Geophys. Res.*, this issue.

Lee, Y.-N., and X.-L. Zhou, Methods for the determination of some soluble atmospheric carbonyl compounds, *Environ. Sci. Technol.*, *27*, 749–756, 1993.

Li, S.-M., and L. A. Barrie, Biogenic sulfur aerosol in the Arctic troposphere, 1, Contributions to total sulfate, *J. Geophys. Res.*, *98*, 20,613–20,622, 1993.

Li, S.-M., and J. W. Winchester, Water soluble organic constituents in Arctic aerosols and snow pack, *Geophys. Res. Lett.*, *20*, 45–48, 1993.

Li, S.-M., and J. W. Winchester, Particle size distribution and chemistry of late winter Arctic aerosols, *J. Geophys. Res.*, *95*, 13,897–13,908, 1990.

Li, S.-M., L. A. Barrie, and D. Toom, Seasonal variations of methanesulfonate, non-sea-salt sulfate, and sulfur dioxide at three sites in Canada, *J. Geophys. Res.*, *101*, 4165–4173, 1996.

Lide, D. R., *CRC Handbook of Chemistry and Physics*, 73rd ed., CRC Press, Boca Raton, Fla., 1992.

Liu, P. S. K., W. R. Leaitch, C. M. Banic, S.-M. Li, D. Ngo, and W. J. Megaw, Aerosol observations at Chebogue Point during NARE 1993: Relationships among CCN, size distribution and chemistry, *J. Geophys. Res.*, this issue.

Novakov, T., and J. E. Penner, Large contribution of organic aerosols to cloud-condensation-nuclei concentrations, *Nature*, *365*, 823–826, 1993.

Olson, M. P., K. K. Oikawa, and A. W. Macafee, A trajectory model applied to the long-range transport of air pollutants: A technical description and some model intercomparisons, *Int. Rep. LRTAP 78-4*, Atmos. Environ. Serv., Downsview, Ont., Canada, 1978.

Penner, J. E., Effect of biomass burning on global radiation budget (abstract), *Eos Trans. AGU*, *73*(14), 71, 1992.

Penner, J. E., R. J. Charlson, J. M. Hales, N. S. Laulainen, R. Leifer, T. Novakov, J. Ogren, L. F. Radke, S. E. Schwartz, and L. Travis, Quantifying and minimizing uncertainty of climate forcing by anthropogenic aerosols, *Bull. Am. Meteorol. Soc.*, *75*, 375–400, 1994.

Radar, D. J., and V. A. Marple, A study of the effects of anisokinetic sampling, *Aerosol Sci. Technol.*, *8*, 283–299, 1988.

Schneider, S. H., Detecting climatic change signals: Are there any "fingerprints"?, *Science*, *263*, 341–347, 1994.

Strapp, J. W., W. R. Leaitch, and P. S. K. Liu, Hydrated and dried aerosol-size-distribution measurements from the Particle Measuring Systems FSSP-300 probe and the deiced PCASP-100X probe, *J. Atmos. Oceanic Technol.*, *9*, 548–555, 1992.

Talbot, R. W., M. O. Andreae, H. Berresheim, P. Artaxo, M. Garstang, R. C. Harriss, K. M. Beecher, and S.-M. Li, Aerosol chemistry during the wet season in central Amazonia: The influence of long-range transport, *J. Geophys. Res.*, *95*, 16,955–16,969, 1990.

Wyslouzil, B. E., K. L. Carleton, D. A. Sonnenfroh, and W. T. Rawlins, Observation of hydration of single, modified carbon aerosols, *Geophys. Res. Lett.*, *21*, 2107–2110, 1994.

C. M. Banic, G. A. Isaac, W. R. Leaitch, Shao-Meng Li (corresponding author), and P. S. K. Liu, Atmospheric Environment Service, 4905 Dufferin Street, Downsview, Ontario M3H 5T4, Canada.

Y.-N. Lee and X.-L. Zhou, Brookhaven National Laboratory, Upton, NY 11973.

(Received June 1, 1995; revised January 16, 1996; accepted January 16, 1996.)